

Simultaneous optical measurements of cell motility and growth

Shamira Sridharan,^{1,2} Mustafa Mir,^{1,3} and Gabriel Popescu^{1,2,3,*}

¹Quantitative Light Imaging Laboratory, Beckman Institute for Advanced Science & Technology, 405 N. Matthews Ave., Urbana, IL 61801, USA.

²Department of Bioengineering, University of Illinois at Urbana Champaign, 1304 Springfield Ave., Urbana, IL 61801, USA.

³Department of Electrical and Computer Engineering, University of Illinois at Urbana Champaign, 619 S. Wright Street, Urbana, IL 61801, USA.

*gpopescu@illinois.edu

Abstract: It has recently been shown that spatial light interference microscopy (SLIM) developed in our laboratory can be used to quantify the dry mass growth of single cells with femtogram sensitivity [M. Mir et al., Proc. Nat. Acad. Sci. **108**, 32 (2011)]. Here we show that it is possible to measure the motility of single cells in conjunction with the dry mass measurements. Specifically the effect of poly-L-lysine substrate on the dry mass growth of *Drosophila* S2 cells is studied. By measuring the mean square displacement of single cells and clusters it is shown that cells that adhere better to the surface are unable to grow. Using such a technique it is possible to measure both growth and morphogenesis, two of the cornerstones of developmental biology.

© 2011 Optical Society of America

OCIS codes: (180.3170) Interference microscopy; (170.1420) Biology; (170.1530) Cell analysis; (170.3880) Medical and biological imaging

References and links

1. W. K. Purves, *Life, the Science of Biology* (Sinauer Associates, W.H. Freeman and Co., Sunderland, Mass., 2004).
2. S. L. Rogers, U. Wiedemann, N. Stuurman, and R. D. Vale, "Molecular requirements for actin-based lamella formation in *Drosophila* S2 cells," *J. Cell Biol.* **162**(6), 1079–1088 (2003).
3. A. Tzur, R. Kafri, V. S. LeBleu, G. Lahav, and M. W. Kirschner, "Cell growth and size homeostasis in proliferating animal cells," *Science* **325**(5937), 167–171 (2009).
4. G. Reshes, S. Vanounou, I. Fishov, and M. Feingold, "Cell shape dynamics in *Escherichia coli*," *Biophys. J.* **94**(1), 251–264 (2008).
5. M. Godin, F. F. Delgado, S. Son, W. H. Grover, A. K. Bryan, A. Tzur, P. Jorgensen, K. Payer, A. D. Grossman, M. W. Kirschner, and S. R. Manalis, "Using buoyant mass to measure the growth of single cells," *Nat. Methods* **7**(5), 387–390 (2010).
6. A. K. Bryan, A. Goranov, A. Amon, and S. R. Manalis, "Measurement of mass, density, and volume during the cell cycle of yeast," *Proc. Natl. Acad. Sci. U.S.A.* **107**(3), 999–1004 (2010).
7. K. Park, L. J. Millet, N. Kim, H. Li, X. Jin, G. Popescu, N. R. Aluru, K. J. Hsia, and R. Bashir, "Measurement of adherent cell mass and growth," *Proc. Natl. Acad. Sci. U.S.A.* **107**(48), 20691–20696 (2010).
8. R. Barer, "Interference microscopy and mass determination," *Nature* **169**(4296), 366–367 (1952).
9. B. Rappaz, E. Cano, T. Colomb, J. Kühn, C. Depeursinge, V. Simanis, P. J. Magistretti, and P. Marquet, "Noninvasive characterization of the fission yeast cell cycle by monitoring dry mass with digital holographic microscopy," *J. Biomed. Opt.* **14**(3), 034049 (2009).
10. R. J. Sokol, J. Wales, G. Hudson 2nd, D. Goldstein, and N. T. James, "Cellular dry mass during macrophage development in malignant lymphoma," *Anal. Quant. Cytol. Histol.* **13**(6), 379–382 (1991).
11. A. F. Brown and G. A. Dunn, "Microinterferometry of the movement of dry matter in fibroblasts," *J. Cell Sci.* **92**(3), 379–389 (1989).
12. N. T. Shaked, J. D. Finan, F. Guilak, and A. Wax, "Quantitative phase microscopy of articular chondrocyte dynamics by wide-field digital interferometry," *J. Biomed. Opt.* **15**(1), 010505 (2010).
13. R. Barer, "Refractometry and interferometry of living cells," *J. Opt. Soc. Am.* **47**(6), 545–556 (1957).
14. R. Barer and K. A. Ross, "Refractometry of living cells," *J. Physiol.* **118**(2), 38P–39P (1952).
15. R. Barer and S. Tkaczyk, "Refractive index of concentrated protein solutions," *Nature* **173**(4409), 821–822 (1954).
16. G. Popescu, Y. Park, N. Lue, C. Best-Popescu, L. Deflores, R. R. Dasari, M. S. Feld, and K. Badizadegan, "Optical imaging of cell mass and growth dynamics," *Am. J. Physiol. Cell Physiol.* **295**(2), C538–C544 (2008).

17. Z. Wang, L. Millet, M. Mir, H. Ding, S. Unarunotai, J. Rogers, M. U. Gillette, and G. Popescu, "Spatial light interference microscopy (SLIM)," *Opt. Express* **19**(2), 1016–1026 (2011).
18. Z. Wang and G. Popescu, "Quantitative phase imaging with broadband fields," *Appl. Phys. Lett.* **96**(5), 051117 (2010).
19. M. Mir, Z. Wang, Z. Shen, M. Bednarz, R. Bashir, I. Golding, S. G. Prasanth, and G. Popescu, "Optical measurement of cycle-dependent cell growth," *Proc. Natl. Acad. Sci. U.S.A.* **108**(32), 13124–13129 (2011).
20. R. Barer, "Determination of dry mass, thickness, solid and water concentration in living cells," *Nature* **172**(4389), 1097–1098 (1953).
21. F. Dubois, C. Schockaert, N. Callens, and C. Yourassowsky, "Focus plane detection criteria in digital holography microscopy by amplitude analysis," *Opt. Express* **14**(13), 5895–5908 (2006).
22. A. Eldar and M. B. Elowitz, "Functional roles for noise in genetic circuits," *Nature* **467**(7312), 167–173 (2010).

1. Introduction

The fundamental processes of developmental biology are *cell differentiation*, *cell growth*, and *morphogenesis* [1]. Differentiation is responsible for the specialization of cell types, growth for increasing the cell population and morphogenesis ("beginning of shape") is responsible for the spatial and temporal organization that gives an organism its complex three-dimensional structure. To achieve morphogenesis *motility* is crucial as it enables cells to position themselves in space and time before undergoing growth or differentiation [2]. Thus, to understand a proliferating cellular system, both growth and motility measurements are necessary.

The traditional and ubiquitous method for measuring cell growth involves using impedance counters to acquire size distributions combined with tedious mathematical analysis of the population level statistics [3]. For some simple organisms such as *Escherichia coli* (*E. coli*) and yeast, traditional microscopy techniques may also be used, given that the density of the cell remains constant through its lifecycle [4]. The reason that no major advances in technique were made for several decades may be attributed to the fact that cells are small, on the scale of picograms and microns, and only double their size during their lifecycle. It has been calculated that in order to answer the simple question of whether the cells are growing exponentially or linearly, a resolution of less than 6% in cell size is required [3]. This requirement translates into sub-picogram mass resolution and sub-micron in size. Additional constraints to these measurements are due to the fact that cells are highly motile and morphologically dynamic.

Despite these massive challenges there has recently been a renewed interest in measuring cell growth and several methods have emerged. One approach is to measure changes in the resonant frequency of vibrating micro channels to determine the buoyant mass of non-adherent cells flowing through them. Due to the transient nature of the measurement, this technology is unable to track single, adherent cells [5,6]. This principle of micro resonators was later extended to measure adherent cells but at the expense of sensitivity and throughput, i.e., only one cell can be measured at a time [7]. Due to these limitations the micro resonator approaches are unable to completely characterize the effects of spatial and temporal interactions between cells on growth and are thus unsuitable for studying motility and morphogenesis.

The other line of emerging technologies for measuring cell mass relies on optical interferometry. The fundamentals of using interferometry to measure dry mass were laid out in the 1950's [8]. The major realization, enabled by phase contrast microscopy, was that the optical phase shift accumulated through a cell is linearly proportional to non-aqueous content or dry mass of the cell. Over the past half century this method has been utilized by many groups to monitor cell dry mass [9–12]. An uncertainty arises in this method when considering the refractive increment, which according to intuition should vary when considering the heterogeneous and complex environment of a cell's interior. However, previous measurements have shown that this value varies less than 5% across a range of biological molecules [8,13–15]. Recently, it has also been shown theoretically and experimentally that small osmotic changes do not affect the surface integral of a quantitative phase map, establishing that quantitative phase imaging can be used to accurately measure dry mass [16]. The reason that this approach hasn't found wider spread yet is largely due to two

reasons: the loss of contrast from speckle generated by highly coherent sources and the complex and often impractical experimental setups required.

To address these issues we have recently developed Spatial Light Interference Microscopy (SLIM) [17,18] which combines traditional phase contrast microscopy with holography. Due to the short coherence length of the white light illumination SLIM images are speckle free and are inherently low noise. SLIM has path length sensitivities of 0.3 nm spatially and 0.03 nm temporally which translates to spatial and temporal dry mass sensitivities of 1.5 fg/ μm^2 and 0.15 fg/ μm^2 respectively. Recently we used SLIM to quantify with femtogram accuracy, the dry mass growth of both *E. coli* and the mammalian U2OS cell line [19]. In *E. Coli* we found evidence of exponential growth and constant density. More importantly, by combining the phase information with fluorescence measurements, we were able to measure the growth dependence on the cell cycle. Using this method we found that U2OS cells grow fastest in the G2 stage of the cell cycle in an exponential manner [19].

Here we show, for the first time to our knowledge, that due to the imaging nature of SLIM we can simultaneously measure the effects of cell motility on growth. In order to prove the utility of the method, we characterize the effects of a *poly-L-lysine substrate* on the growth of S2 *Drosophila* cells. Our results indicate that this technique can be used to study many spatial-temporal interactions across any type of cell line. This approach will ultimately enable us to quantitatively address questions about two of the cornerstones of developmental biology: *growth and morphogenesis*.

2. Materials and methods

Drosophila Schneider S2 cells (Invitrogen, R690-07) were passaged every four days with Schneider's Insect Medium (Sigma-Aldrich, S9895), and were transferred onto a glass bottom dish (MatTek, P35G-1.0) coated with 0.01% poly-L-lysine (Sigma-Aldrich, P8920) 24 hours after passaging. Prior to coating with poly-L-lysine (PLL) the dish was washed with distilled water and ethanol. The PLL was aspirated after 30 minutes and was allowed to air dry after which the dish was sterilized under UV light. The cells were allowed to settle on the PLL substrate for an hour prior to imaging.

Imaging was performed using SLIM, which is described in more detail in Refs. [17,18]. In short, SLIM is built as an add-on module to a commercial inverted phase contrast microscope (Zeiss Axio Observer Z1) and operates by imparting additional spatial modulation to the image field. For conventional phase contrast microscopy, the phase objective contains a phase ring that imparts a $\pi/2$ phase shift to the un-scattered light relative to the scattered light. For SLIM, the back focal plane of the phase contrast objective is projected onto a liquid crystal phase modulator (LCPM). The LCPM introduces 3 additional phase shifts in increments of $\pi/2$ to the un-scattered light, corresponding to 4 intensity images. From the four intensity maps, a uniquely determined quantitative phase image is reconstructed. SLIM time lapse images were acquired using the Zeiss EC Plan-Neofluar 10x/0.3 Ph1 objective. As previously shown [19] the low numerical aperture of the objective ensures that the phase measured is integrated over the entire depth of the cell. The sample was scanned every 10 minutes in a 2x2 mosaic providing a total field of view of 0.67 x 0.50 mm². At each location in the mosaic, a 10 slice z-stack was also acquired with a slice spacing of 4.8 μm . The total acquisition time was 47 hours, sufficient to capture dry mass growth data from four generations of cells.

The dry mass density ($\text{pg}/\mu\text{m}^2$) at each pixel is calculated as

$$\rho(x, y) = \lambda\phi(x, y) / 2\pi\gamma, \quad (1)$$

where $\gamma = 0.2$ ml/g is the refractive increment of protein [8,16,19,20] and ϕ is the measured phase in radians. To further ensure that the total dry mass is captured over the entire depth of the cell, the projected maximum of the 5 slices around the center of the z-stack is used to calculate the dry mass density map. The center of the stack was determined by identifying the slice of maximum phase value [21]. It is important to note that even though the average refractive increment may vary across different cell types, this would only affect the absolute

value of the dry mass and not the conclusions drawn from the growth trends. To retrieve single cell and cluster data, the images were manually segmented using the ROI manager in ImageJ (NIH) and a tablet interface. Once ROI's are obtained, geometrical parameters such as area, perimeter and circularity are readily available. From the measured projected area the total dry mass of the cell is calculated by integrating over the ROI. Finally, a running average on the dry mass data is performed with a window of 50 minutes.

In addition, the cell mass centroid position measurements are used to calculate the mean square displacements, MSD,

$$\begin{aligned} MSD(\tau) &= \left\langle [\mathbf{r}(t+\tau) - \mathbf{r}(t)]^2 \right\rangle_t \\ &= \left\langle [x(t+\tau) - x(t)]^2 \right\rangle_t + \left\langle [y(t+\tau) - y(t)]^2 \right\rangle_t, \end{aligned} \quad (2)$$

where $|\mathbf{r}(t+\tau) - \mathbf{r}(t)|$ is the mean distance travelled by the cell over the time interval τ and angular brackets denote time averaging. For this study 4 cells were tracked in the 1st generation, and 2 each in the 2nd, 3rd and 4th generations. In addition to the single cell tracking, entire cell clusters were also tracked, with 4 clusters in the 3rd generation and 2 clusters in the 4th generation.

3. Results

From the single cell analysis it was found that cells with a lower MSD ($< 10 \mu\text{m}^2$) exhibit low or negative dry mass growth. Figure 1 below shows representative examples of the tracked single cells. In Fig. 1(a) the yellow solid circles indicate the ROIs that were used in each frame and the corresponding mean square displacements are shown in Fig. 1(c). Clearly, the cell associated with the red trace is attached to the glass surface, as the motion is restricted and exhibits very limited motion. This type of motion is reminiscent of the paths taken by particles under Brownian motion.

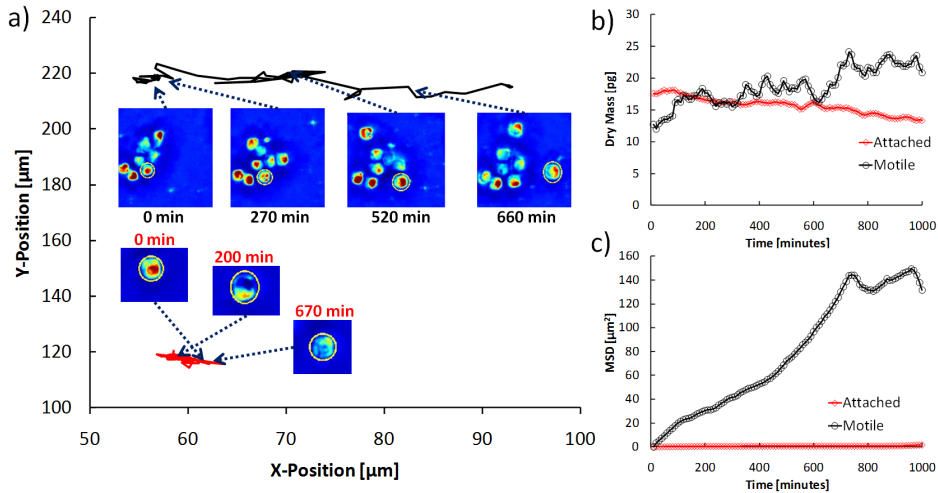


Fig. 1. a) Trajectories of attached (red line) and motile (black line) cells. Time-stamped insets show the tracked cell at various time points. It can be seen that the motile cell exhibits a clear directional motion over time whereas the adherent cell is jostling in place. b) The dry mass growth of the two cells shown in a, the attached cell exhibits no growth whereas the motile cell approximately doubles its mass. c) MSD for the two cells shown in b.

On the other hand the motile cell (black trace) exhibits a clear directional motion over time. The corresponding dry mass curves in Fig. 1(b) show that the attached cell exhibits negative growth whereas the motile cell has clear positive growth, though the data is much noisier. This noise may be attributed to three major reasons. First, in the unattached cells we

can expect greater dynamic rearrangements of the actin cytoskeleton (even though S2 cells don't exhibit any clear polarity) [2]. This will likely cause spontaneous changes in the cell dry mass, which to our knowledge has never been measured or characterized. Secondly, the cell motility increases with each generation, which means that contribution to the noise from accumulated cellular debris and numerical segmentation is greater in these cells. Third, as the motile cells are healthier from their growth, it can be expected that normal cellular activity and thus natural biological noise [19,22] in these cells will also be greater relative to the attached cells. The measurement of the normal levels of biological noise is also of great scientific interest as it may reveal the nature of the underlying regulatory systems. The underlying idea here is that proteins are not produced at uniform rates, rather, due to the stochastic nature of RNA translation, the production occurs in a more burst like manner [22].

The MSD analysis also allows us to measure how the poly-L-lysine affects cell growth over time. Figure 2(a) shows that the MSD increases by 4 orders of magnitude between the 1st and 4th generations. In order to establish a relationship between the MSD and growth rate, each of the single cell growth curves was fit with a linear function. It was found that the average correlation coefficient (R^2) for both linear and exponential fittings is 0.663. Figure 2(b) compares the maximum MSD for each cell with its fitted linear growth rate showing that the MSD and growth rate are related in an exponential manner.

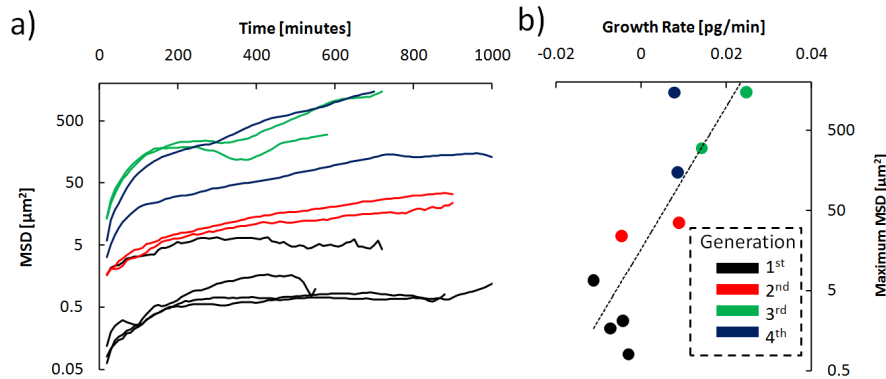


Fig. 2. a) Semilogarithmic plot MSD vs. time for all the individual cells tracked. It can be seen that the MSD increases by 3-4 orders of magnitude between the 1st and 4th generations b) Semilogarithmic plot of the maximum MSD vs. the approximated linear growth rate for each cell.

Although the limited single cell data is not enough to differentiate between exponential and linear growth, entire cell clusters were analyzed to measure the bulk growth properties of the S2 cells. From the MSD analysis discussed above it is clear that the cells only begin to grow normally once they are completely non-adherent, starting from the 3rd generation (Fig. 3). Thus to determine the normal growth pattern, 4 cell clusters in the 3rd generation and 2 cell clusters in the 4th generation were analyzed. Each of the cluster growth curves were fit to an exponential function (solid black lines in Fig. 3) $M(t) = M_0 e^{t/\tau_0}$. The average time constant measured, τ_0 , was found to be 240.4 and 364.4 minutes for the 3rd and 4th generations, respectively.

4. Conclusions

By studying the relationship between a single cell's MSD and growth rate we have shown that S2 cells will not grow normally when attached to a poly-L-lysine substrate. However, the effects of the poly-L-lysine wear off by the 3rd generation of cells, after which the cells exhibit normal growth trends as quantified by the measurements on cell clusters. Poly-L-lysine promotes cell adhesion through electrostatic interactions, specifically by increasing the number of positively charged sites available on the substrate, to which the negatively charged

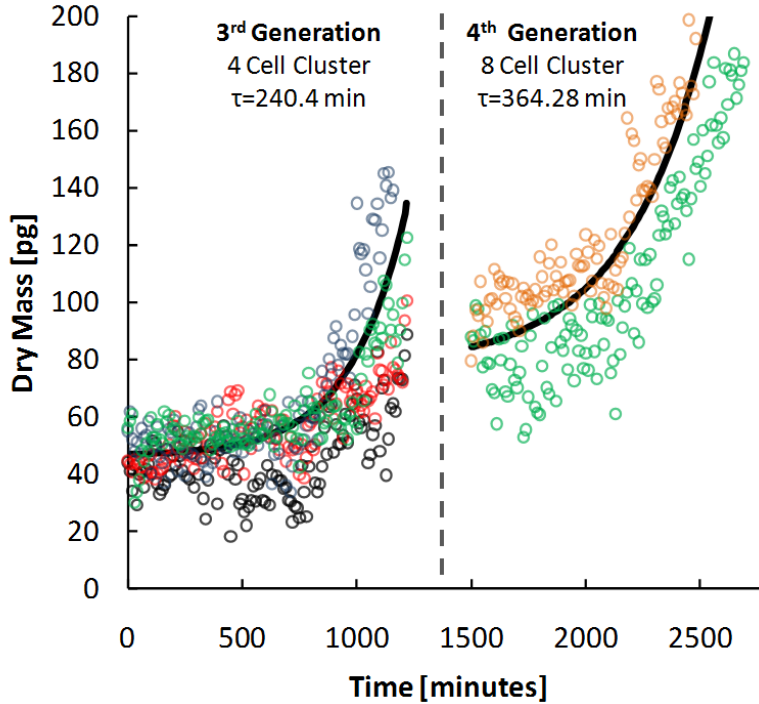


Fig. 3. Dry mass vs. time for cell clusters in the 3rd and 4th generations. Each colored time series corresponds to a single cluster, the solid black line is the average exponential fit for each cluster, with the average time constant, τ shown for each fit.

ions on the cell membrane bind. After several generations it is likely that these sites are saturated by negative ions in the culture media when the substrate is treated with low concentration of poly-L-lysine. Thus, adhesion is proportional to the concentration of binding sites. Our measurements on S2 growth on substrates treated with higher concentrations of poly-L-lysine (data not shown) indicate that its effects do not wear off even after 4 generations. This seems to confirm that the saturation effect of the adhesion is related to the concentration of available binding sites. The technology and analysis developed here can be extended to study the effects of spatial and temporal interactions on cell growth in a proliferating culture. This type of study may answer important questions regarding both cell growth and morphogenesis and is currently not possible using any other method.

Acknowledgments

The S2 cells and media were kindly provided by Benjamin Blehm and Paul Selvin (University of Illinois at Urbana-Champaign). This research was supported in part by the National Science Foundation (grants CBET 09-46660 CAREER, CBET-1040462 MRI, CBET-0939511). For more information, visit <http://light.ece.uiuc.edu/>.